

The GTP-Binding Protein Septin 7 Is Critical for Dendrite Branching and Dendritic-Spine Morphology

Yunli Xie,¹ John P. Vessey,¹ Anetta Konecna,¹
Ralf Dahm,¹ Paolo Macchi,^{1,2,*}
and Michael A. Kiebler^{1,*}

¹Department of Neural Cell Biology
Center for Brain Research
Medical University of Vienna
Vienna A1090
Austria

Summary

Septins, a highly conserved family of GTP-binding proteins, were originally identified in a genetic screen for *S. cerevisiae* mutants defective in cytokinesis [1, 2]. In yeast, septins maintain the compartmentalization of the yeast plasma membrane during cell division by forming rings at the cortex of the bud neck, and these rings establish a lateral diffusion barrier. In contrast, very little is known about the functions of septins in mammalian cells [3, 4] including postmitotic neurons [5–7]. Here, we show that Septin 7 (Sept7) localizes at the bases of filopodia and at branch points in developing hippocampal neurons. Upon downregulation of Sept7, dendritic branching is impaired. In mature neurons, Sept7 is found at the base of dendritic spines where it associates with the plasma membrane. Mature Sept7-deficient neurons display elongated spines. Furthermore, Sept5 and Sept11 colocalize with Sept7 and coimmunoprecipitate with Sept7, thereby arguing for the existence of a Septin5/7/11 complex. Taken together, our findings show an important role for Sept7 in regulating dendritic branching and dendritic-spine morphology. Our observations concur with data from yeast, in which downregulation of septins yields elongated buds, suggesting a conserved function for septins from yeast to mammals.

Results and Discussion

We initially investigated whether Sept7 expression is developmentally regulated in hippocampal neurons. Western-blot analysis of proteins extracted from neurons at different days in vitro (DIV) with a specific, immunopurified anti-Sept7 antibody [8] revealed that Sept7 is expressed at all stages of neuronal differentiation [9] (Figure 1A). However, expression increases significantly after 3 DIV when dendritic outgrowth begins, suggesting a role for Sept7 in dendrite morphogenesis. To investigate the subcellular localization of Sept7 in both developing and mature neurons, we performed

immunostainings on cultured hippocampal neurons. In stage 2 neurons, Sept7 is detected in all neurites (data not shown). Sept7 is particularly enriched in the proximal part of growth cones where it is present within F-actin bundle-rich areas (Figure 1B). In developing processes, Sept7 is not homogeneously distributed but rather found in patches at the plasma membrane (Figure 1B, arrowheads), often at the base of filopodia and at branch points. In mature dendrites (Figure 1C), Sept7 preferentially forms discrete arc-shaped clusters (arrowheads) that do not enter the protrusions. In mature neurons, Sept7 is present both in the somatodendritic compartment as well as in axons (Figure 1D) and is highly enriched in presynaptic axon terminals (data not shown). To investigate whether Sept7 is found at or near synapses, we performed costaining against Sept7 and PSD95 (Figure 1E, upper panels). Interestingly, Sept7 staining does not colocalize with that of PSD95 as previously reported [7]. When dendritic spines, visualized by phalloidin staining, are found nearby, Sept7 forms arc-shaped clusters around the base of the spine. In some cases, ring-like structures are observed (Figure 1E, middle and lower panels, arrowheads). These structures are reminiscent of the pattern observed during cell division at the yeast's bud neck, where septins form ring-like structures [10], suggesting that the septins might have similar functions in yeast and mammalian neurons.

Septins have been previously reported to form heterooligomeric complexes. For example, a Sept2/6/7 complex has been identified in HeLa cells [11], whereas in fibroblasts, a Sept7/9b/11 complex has been characterized [12]. To test whether other septins show a similar subcellular localization as shown by Sept7 in neurons and whether they might be found in a common complex, we performed immunostaining on cultured hippocampal neurons by using antibodies against Sept2, Sept5, Sept8, Sept9, and Sept11. Although Sept2 is highly expressed in glia, its expression in hippocampal neurons is negligible (Figure S1A in the Supplemental Data available online). Sept8, like Sept7, is present in the cell body, in axons, and in dendrites. However, its staining pattern resembles intracellular vesicles and not that of Sept7 in dendrites (Figure S1B and data not shown). Sept9 is expressed in hippocampal neurons; however, the staining pattern for Sept9 with three different Sept9 antisera is clearly distinct from that of Sept7 (data not shown).

Sept5 and Sept11 are expressed both in the cell body and dendrites; those staining patterns are very reminiscent to that of Sept7 (Figures 2A and 2B and Figure S1C). To examine whether Sept5 and Sept11 indeed interact with Sept7, we performed immunoprecipitation experiments by using Sept7 or Sept11 antibodies (Figure 2C). The anti-Sept11 antibody efficiently coimmunoprecipitates Sept5 and Sept7, and the anti-Sept7 antibody coimmunoprecipitates Sept5. Taken together, these data argue for the existence of a Sept5/7/11 complex in neuronal dendrites. We cannot exclude, however, that other Sept7 complexes might exist. It is interesting to

*Correspondence: macchi@science.unitn.it (P.M.), michael.kiebler@meduniwien.ac.at (M.A.K.)

²Present address: Center for Integrative Biology, Laboratory of Molecular and Cellular Neurobiology, University of Trento, 38060 Trento, Italy.

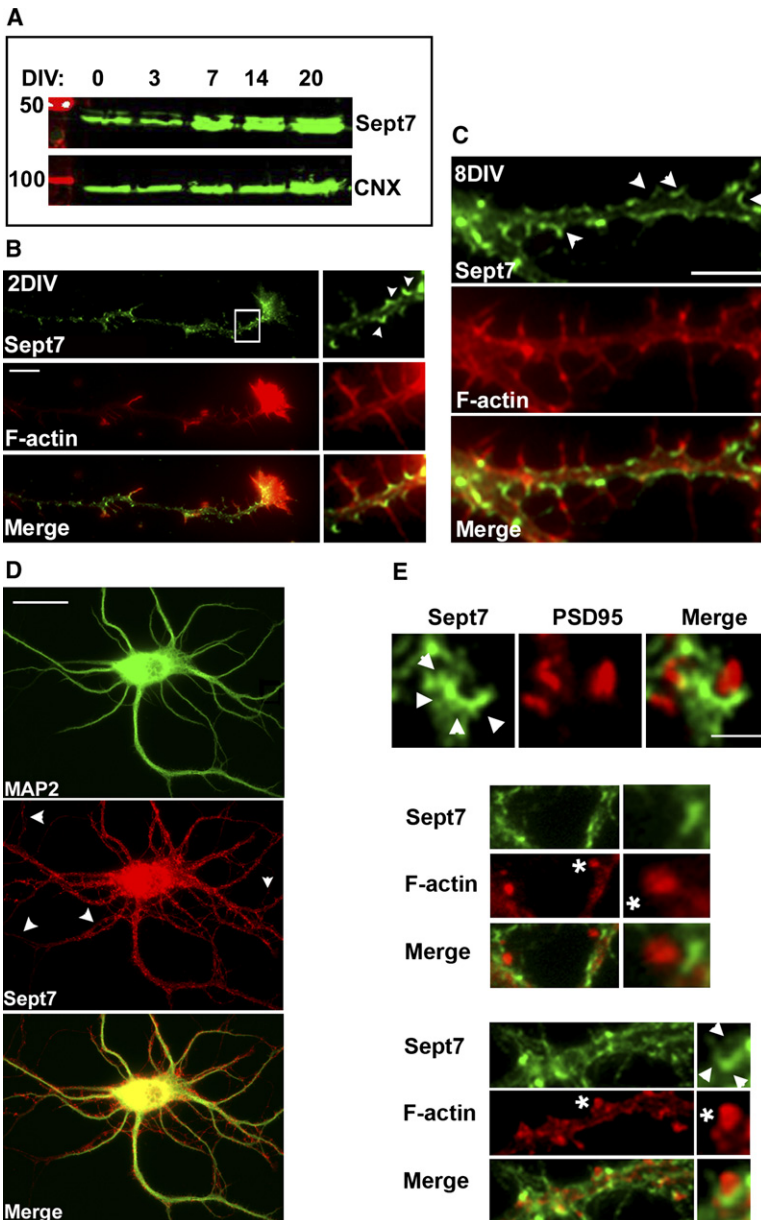


Figure 1. Subcellular Localization of Sept7 Protein in Neurons

(A) Western-blot analysis showing Sept7 expression in hippocampal neurons at different DIV. Calnexin (CNX) served as loading control. The numbers “50” and “100” represent molecular weight markers of 50 and 100 kDa, respectively.

(B) Sept7 localization in developing (2DIV) hippocampal neurons by immunostaining. High-magnification insets show that Sept7 (green) localizes at the bases of filopodia (insets, arrowheads) visualized by phalloidin (red). The scale bar represents 50 μ m.

(C) Sept7 (arrowheads) localizes at the bases of protrusions and branch points in mature (8 DIV) dendrites. The scale bar represents 10 μ m.

(D) Sept7 (red) is found in MAP2-positive (green) dendrites. Arrowheads indicate the MAP2-negative mature axons that are stained for Sept7. The scale bar represents 100 μ m.

(E) Sept7 localizes at the bases of dendritic spines (asterisks) of 21 DIV neurons. Costaining of Sept7 (green) and either PSD95 (upper panels) or F-actin (both red, middle and lower panels) are shown. Note the ring-like structures formed by Sept7 surrounding the bases of dendritic spines (arrowheads). The scale bar represents 2 μ m.

note in this context that several mammalian septins might be interchangeable in septin complexes. It has, for example, been shown that in a Sept2/6/7 complex, Sept2 can be replaced by Sept5 (or Sept1 or Sept4) and Sept6 by Sept11 (or possibly by Sept8 or Sept10) [13]. Therefore, a Sept5/7/11 complex is not in contradiction with the previously reported Sept2/6/7 or Sept7/9b/11 complexes.

We next investigated in more detail the intracellular localization of Sept7. Septin H5 (Sept4), another member of the septin family, was previously shown to associate with the plasma membrane via a polybasic motif of 7 amino acids (HRKSVKK) [14]. A similar seven amino acid motif is also present near the GTP-binding domain in all Sept7 orthologs (Figure S2). When hippocampal neurons were permeabilized with 0.2% Triton X-100, Sept7 immunoreactivity is greatly reduced, indicating that Sept7 is associated with the plasma membrane in this cell type (data not shown). We next fractionated

rat brain homogenates by differential centrifugation to obtain a cytoskeleton-containing membrane pellet (P) and a soluble protein supernatant (S) (Figure 2D). The P fraction was then incubated twice with 1% Triton X-100, and this was followed by a centrifugation step for separating solubilized transmembrane and membrane-associated proteins from cytoskeletal components. Under these conditions, the majority of Sept7 is retrieved in the Triton-soluble fraction (P/s, P/s’) together with calnexin and synaptophysin, whereas only a small fraction of Sept7 cosediments with insoluble β -actin (P/p’). These results indicate that Sept7 is primarily associated with membranes. We cannot, however, exclude that a fraction of Sept7 might be associated with the cytoskeleton.

Because Sept7 is found at the bases of neuronal protrusions, we hypothesized that it might play an important role in maintaining both the structure of branch points and the morphology of protrusions in neurons.

Septin 7 and Dendritic Protrusions

3

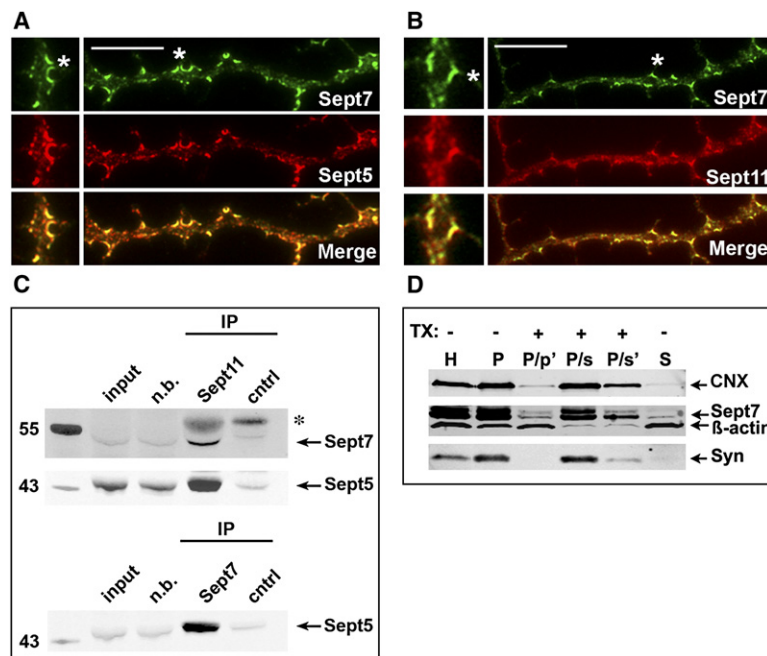


Figure 2. Sept7 Colocalizes with Sept5 and Sept11 in Cultured Hippocampal Neurons and Is Associated with the Plasma Membrane (A and B) In 6 DIV neurons, Sept5 and Sept11 (both in red) enrich at the bases of filopodia (enlargements), and at these bases, they colocalize with Sept7 (green). Scale bars represent 10 μ m.

(C) Coimmunoprecipitation of Sept5, Sept7, and Sept11 from adult rat brain. Immunoprecipitations (IP) were performed with anti-Sept7, anti-Sept11 antibodies or preimmune sera (control). Immunoprecipitates were probed for the presence of Sept5 and Sept7 by western blotting. “n.b.” stands for non-bound after IP; “cntrl” stands for control; and “55” and “43” stands for molecular weight markers of 55 and 43 kDa, respectively.

(D) Sept7 is membrane associated in the adult rat brain. Membrane (P) and soluble protein fractions (S) were obtained by differential centrifugation of a rat brain homogenate (H). Sept7 is found predominantly in detergent-soluble fractions (P/s and P/s’) together with the membrane protein markers, calnexin (CNX), and synaptophysin (Syn). β -actin is enriched in the detergent-insoluble fraction. “TX” stands for Triton X-100.

We tested this hypothesis by using RNAi to downregulate Sept7 in neurons. Dissociated primary hippocampal neurons were transfected by nucleoporation [15, 16] with pSuperior plasmids expressing short hairpin RNAs (shRNA) that target Sept7 (termed shSept7). As negative controls, plasmids encoding a mismatch Sept7 shRNA or a shRNA against a nonexpressed mRNA (shRFP) were used (Figure 3A). Furthermore, neurons were also transfected with an empty pSuperior vector (data not shown). The level of Sept7 downregulation in cultured neurons was determined by western-blot analysis. shSept7 significantly downregulated Sept7 protein expression, whereas none of the controls had any effect on Sept7 expression levels (Figure 3A). Sept7 downregulation in neurons was also confirmed by immunostaining of shRNA-treated neurons with anti-Sept7 antibodies (Figure S3A).

We next investigated whether Sept7 downregulation affects the expression of other septins, notably those that we found to colocalize with Sept7 in dendrites (see Figure 2). Interestingly, both Sept5 and Sept11 expression levels were diminished in Sept7-deficient neurons (Figure 3B). This correlates with previous findings in which Sept7 is significantly diminished in homozygotic Sept5 (CDCrel-1) null mice [17]. Our findings further support the presence of a Sept5/7/11 complex in neurons and confirms previous results that downregulation of one septin affects the expression of other septin-complex members [8, 11].

For assessing the effect of the downregulation of Sept7 on dendritic outgrowth in cell culture, hippocampal neurons were transiently transfected with plasmids described below at 4 DIV and fixed after 3 days of expression. Neurons expressing shSept7 show a simplified dendritic tree with a reduction in branching (Figure 3C). To quantify this reduction, we performed a Sholl analysis [18]. Here, the number of dendritic crossings of concentric circles at various radial distances from the cell body is counted. In neurons transfected with either an empty

pSuperior vector expressing GFP or a vector expressing a control shRNA (shRFP), the number of dendritic line crossings increases with the distance from the cell body and reaches a peak at approximately 30–40 μ m, after which it begins to decrease (Figure 3D). In shSept7-transfected neurons, we found a nearly 2-fold reduction in the number of line crossings for all radial distances. Similar results were obtained with a second vector expressing a shRNA targeting a different region of the sept7 mRNA (shSept7-2) but not with the mismatch Sept7 shRNA, suggesting that the observed phenotype is related to Sept7 downregulation (Figures S3B–S3E). To exclude offtarget effects of the RNAi, we devised several control experiments. First, we tested whether the observed phenotype could be rescued by the overexpression of an RNAi cleavage-resistant sept7 mRNA (Sept7R). The expression of Sept7R rescues the observed phenotype caused by shSept7 to a significant extent (Figures 3C and 3D). Second, we generated a mutant Sept7 (Sept7m) with critical point mutations in the GTP-binding domain [19] (Figure S2). Whereas overexpressed wild-type GFP-tagged Sept7 results in long filaments orientated along microtubules, overexpressed mutated Sept7m does not aggregate, but yields a homogeneous expression pattern in neurons (Figure S4). Similar observations have been reported for Sept2 (Nedd5) [20], in which fiber formation could be disrupted by microinjection of GTP γ S or by the expression of a Sept2 mutant lacking GTP-binding activity. These data imply that GTP binding is required for septin filament assembly and possible association with the cytoskeleton. To assess whether mutations in the GTP-binding domain of Sept7 also affect dendritic branching, we expressed Sept7m in developing neurons (Figures 3C and 3D). This caused a significant reduction in dendritic-arbor complexity similar to that observed for Sept7 shRNAs. Taken together, the rescue of the observed phenotype by an RNAi-resistant sept7 mRNA and the expression

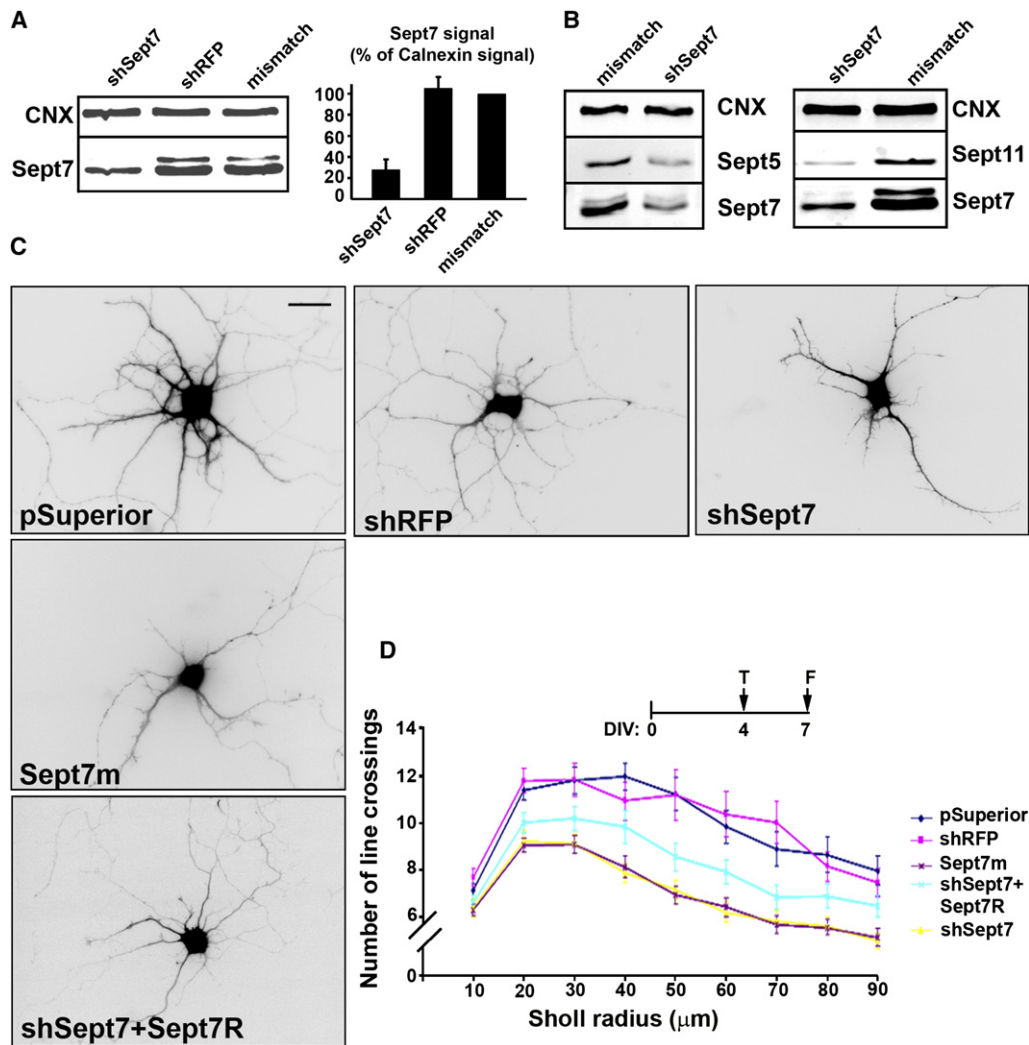


Figure 3. Downregulation of Sept7 Affects Dendritic-Arbor Complexity

(A) Western blot of hippocampal neurons nucleoporated with plasmids expressing shSept7 (lane 1), shRFP (lane 2), and a Sept7 mismatch shRNA (lane 3). Cells were lysed after 3 days of expression and processed for western blotting. The Sept7 level is significantly reduced upon shSept7 expression. The graph shows a quantification of Sept7 downregulation.

(B) Downregulation of Sept7 affects expression levels of Sept5 and Sept11. Neurons were treated as in (A).

(C) Knockdown of Sept7 reduces dendritic arbor complexity. Shown in this panel are representative images of neurons transfected (T) with the following constructs at 4 DIV and fixed (F) 3 days later: (1) empty pSuperior vector; vectors expressing (2) shRFP, (3) shSept7, (4) a mutant Sept7m mRNA or (5) shSept7 cotransfection with Sept7R, a shSept7 cleavage-resistant Sept7, respectively. The scale bar represents 100 μm.

(D) Quantification of dendritic-arbor complexity measured by Sholl analysis. shSept7-treated neurons show significantly fewer line crossings at each radius ($p < 0.001$). The total number of neurons analyzed was 40 for shSept7, 42 for Sept7m, 36 for shSept7+Sept7R, 25 for shRFP, and 33 for pSuperior. Errors bars represent the SEM. Three independent experiments were performed.

of the Sept7 mutant that recapitulates the phenotype observed upon Sept7 downregulation strongly indicate that our shRNAs specifically target *sept7* mRNA. Moreover, the GTP-binding activity of Sept7 is required for normal branch formation in developing hippocampal neurons.

We further assessed whether the density and the morphology of mature dendritic spines was affected by the loss of Sept7. Neurons expressing a mismatch shRNA display normal mushroom-like dendritic spines characteristic of hippocampal neurons (Figure 4). Upon expression of shSept7, we observed numerous changes in spine morphology. First, there is an increase in protrusions that are longer than 2 μm, with a concomitant decrease in normal spines (typically protruding no more

than 2 μm from the dendritic shaft). There is a small effect in neurons expressing mutant Sept7m; however, this is not significant (Figure 4A). Second, there are also changes in overall protrusion density. Expression of shSept7 causes a small but significant reduction of protrusion density. Expression of Sept7m led to an even greater reduction (Figure 4B). Third, we noticed that dendritic spines from Sept7-deficient neurons or neurons expressing Sept7m also appeared longer, and their heads were larger in diameter than those of control neurons (Figure 4C). The average length of all dendritic spines significantly increases in shSept7-treated neurons and in neurons expressing Sept7m (Figure 4D). In addition, spine heads in Sept7-deficient neurons and Sept7m-expressing neurons are significantly larger

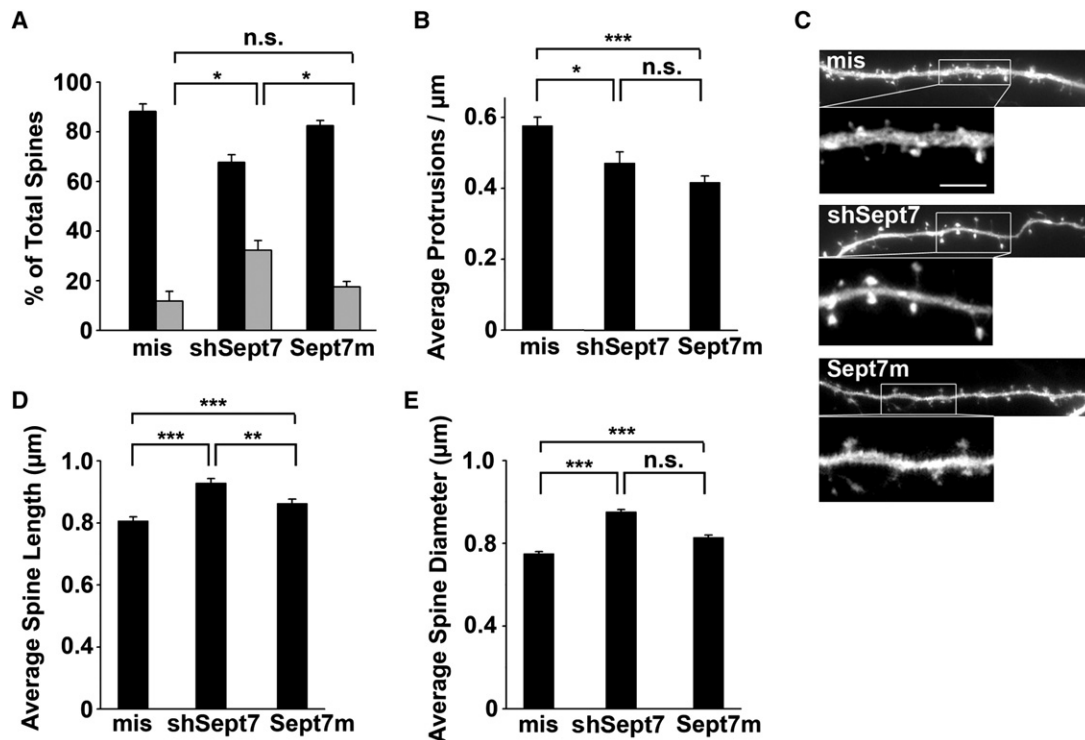


Figure 4. Downregulation of Sept7 Affects Dendritic-Spine Morphogenesis

(A) Neurons transfected at 15 DIV with shSept7 but not with mismatch (mis) display an increase in elongated protrusions that are longer than $2 \mu\text{m}$ ($32.3\% \pm 3.9\%$ SEM versus $11.8\% \pm 3.0\%$ SEM; $p < 0.05$) when they were analyzed 3 days after transfection. Neurons transfected with Sept7m show only a moderate increase in elongated protrusions ($17.6\% \pm 1.2\%$ SEM, n.s.). Black columns represent protrusions less than $2 \mu\text{m}$ long; gray columns represent protrusions longer than $2 \mu\text{m}$.

(B) Neurons transfected with shSept7 or Sept7m, but not with mis, display a significant reduction in the number of protrusions per μm dendrite length (0.47 ± 0.09 SEM or 0.41 ± 0.02 SEM versus 0.58 ± 0.02 SEM). In total, 2014 dendritic spines were analyzed for mis, 1241 were analyzed for shSept7, and 885 were analyzed for Sept7m in (A) and (B).

(C) Representative images of Sept7-deficient and Sept7m-expressing neurons illustrate the increase in both spine length and spine-head diameter. The scale bar represents $5 \mu\text{m}$.

(D) Neurons lacking Sept7 or expressing Sept7m yield elongated dendritic spines. The length of dendritic spines with a mushroom-like head was measured in the control (mis; $1.21 \pm 0.03 \mu\text{m}$ SEM, $n = 471$), shSept7-treated neurons ($1.46 \pm 0.03 \mu\text{m}$ SEM, $n = 734$), and neurons expressing Sept7m ($1.33 \mu\text{m} \pm 0.03$ SEM, $n = 478$).

(E) Neurons lacking Sept7 ($0.95 \pm 0.01 \mu\text{m}$ SEM, $n = 734$) or expressing Sept7m ($0.83 \pm 0.01 \mu\text{m}$ SEM, $n = 478$) show enlarged dendritic-spine heads compared to mismatch-treated neurons (mis; $0.75 \pm 0.01 \mu\text{m}$ SEM, $n = 471$). * $p < 0.05$, ** $p < 0.01$, and *** $p < 0.001$. "n.s." stands for not significant.

(Figure 4E). Taken together, our findings indicate that downregulation of Sept7 as well as overexpression of Sept7m alters the morphology of dendritic protrusions in mature neurons.

In dividing yeast cells, septins seem to play a dual role. First, they are thought to recruit specific protein components to the bud neck. Second, septins have been suggested to form a diffusion barrier that prevents the movement of membrane proteins between the mother cell and the bud [10, 21]. In neurons, Sept7 forms arc-like clusters at the base of filopodia and of dendritic spines, which can also adopt a ring-like shape that resembles the ring structures at the yeast bud neck. When Sept7 is downregulated in neurons, dendritic spines change their shape to form elongated protrusions, reminiscent of the elongated buds in septin-deficient yeast cells [10]. These similarities suggest that Sept7 might fulfill a conserved function in neurons. Similar to the yeast bud neck, it might be a critical component of a diffusion barrier within dendritic spines. Such a function would be the long-sought molecular

correlate for explaining the fact that dendritic spines are distinct compartments and that their motility is important for synaptic plasticity.

Supplemental Data

Experimental Procedures and four figures are available at <http://www.current-biology.com/cgi/content/full/17/20/DC1/>.

Acknowledgments

We thank Sabine Thomas and Martina Schwarz for excellent technical assistance and Dr. Y. Barral and Dr. I. Macara for discussions. We are grateful to the following people for reagents and advice: Dr. M. Kinoshita (Kyoto University, Japan), Dr. K. Nagata (Aichi Human Service Center, Japan), Dr. P. Pasierbek (IMP-IMBA, Vienna, Austria), W. Trimble (University of Toronto, Canada), R. Walikonis (California Institute of Technology, Pasadena, California), and B. Zieger (University of Freiburg, Germany). We thank Dr. T. Tada and Dr. M. Sheng for sharing unpublished reagents and data. This work was supported by the SFB446, the Schram-Foundation, HFSP network, the Hochschuljubiläumsstiftung of the City of Vienna, an initial startup grant from the MUW through Wolfgang Schütz (all to M.A.K.), by a postdoctoral fellowship from the Swiss National

Science Foundation to A.K. and by the Austrian Science Fund (FWF) to P.M.

Received: March 28, 2007

Revised: August 13, 2007

Accepted: August 13, 2007

Published online: October 11, 2007

References

1. Hartwell, L.H. (1971). Genetic control of the cell division cycle in yeast. IV. Genes controlling bud emergence and cytokinesis. *Exp. Cell Res.* **69**, 265–276.
2. Adams, A.E., and Pringle, J.R. (1984). Relationship of actin and tubulin distribution to bud growth in wild-type and morphogenetic-mutant *Saccharomyces cerevisiae*. *J. Cell Biol.* **98**, 934–945.
3. Kinoshita, M., and Noda, M. (2001). Roles of septins in the mammalian cytokinesis machinery. *Cell Struct. Funct.* **26**, 667–670.
4. Spiliotis, E.T., and Nelson, W.J. (2006). Here come the septins: Novel polymers that coordinate intracellular functions and organization. *J. Cell Sci.* **119**, 4–10.
5. Kühlenbaumer, G., Hannibal, M.C., Nelis, E., Schirmacher, A., Verpoorten, N., Meuleman, J., Watts, G.D., De Vriendt, E., Young, P., Stogbauer, F., et al. (2005). Mutations in SEPT9 cause hereditary neuralgic amyotrophy. *Nat. Genet.* **37**, 1044–1046.
6. Hsu, S.C., Hazuka, C.D., Roth, R., Foletti, D.L., Heuser, J., and Scheller, R.H. (1998). Subunit composition, protein interactions, and structures of the mammalian brain sec6/8 complex and septin filaments. *Neuron* **20**, 1111–1122.
7. Walikonis, R.S., Jensen, O.N., Mann, M., Provance, D.W., Jr., Mercer, J.A., and Kennedy, M.B. (2000). Identification of proteins in the postsynaptic density fraction by mass spectrometry. *J. Neurosci.* **20**, 4069–4080.
8. Kinoshita, M., Field, C.M., Coughlin, M.L., Straight, A.F., and Mitchison, T.J. (2002). Self- and actin-templated assembly of mammalian septins. *Dev. Cell* **3**, 791–802.
9. Dotti, C.G., Sullivan, C.A., and Banker, G.A. (1988). The establishment of polarity by hippocampal neurons in culture. *J. Neurosci.* **8**, 1454–1468.
10. Barral, Y., Mermall, V., Mooseker, M.S., and Snyder, M. (2000). Compartmentalization of the cell cortex by septins is required for maintenance of cell polarity in yeast. *Mol. Cell* **5**, 841–851.
11. Kremer, B.E., Haystead, T., and Macara, I.G. (2005). Mammalian septins regulate microtubule stability through interaction with the microtubule-binding protein MAP4. *Mol. Biol. Cell* **16**, 4648–4659.
12. Nagata, K., Asano, T., Nozawa, Y., and Inagaki, M. (2004). Biochemical and cell biological analyses of a mammalian septin complex, Sept7/9b/11. *J. Biol. Chem.* **279**, 55895–55904.
13. Kinoshita, M. (2003). Assembly of mammalian septins. *J. Biochem.* **134**, 491–496.
14. Zhang, J., Kong, C., Xie, H., McPherson, P.S., Grinstein, S., and Trimble, W.S. (1999). Phosphatidylinositol polyphosphate binding to the mammalian septin H5 is modulated by GTP. *Curr. Biol.* **9**, 1458–1467.
15. Zeitelhofer, M., Vessey, J.P., Xie, Y., Tubing, F., Thomas, S., Kiebler, M., and Dahm, R. (2007). High-efficiency transfection of mammalian neurons via nucleofection. *Nat. Protoc.* **2**, 1692–1704.
16. Goetze, B., Tuebing, F., Xie, Y., Dorostkar, M.M., Thomas, S., Pehl, U., Boehm, S., Macchi, P., and Kiebler, M.A. (2006). The brain-specific double-stranded RNA-binding protein Staufen2 is required for dendritic spine morphogenesis. *J. Cell Biol.* **172**, 221–231.
17. Peng, X.R., Jia, Z., Zhang, Y., Ware, J., and Trimble, W.S. (2002). The septin CDCrel-1 is dispensable for normal development and neurotransmitter release. *Mol. Cell Biol.* **22**, 378–387.
18. Sholl, D.A. (1953). Dendritic organization in the neurons of the visual and motor cortices of the cat. *J. Anat.* **87**, 387–406.
19. Versele, M., and Thorer, J. (2004). Septin collar formation in budding yeast requires GTP binding and direct phosphorylation by the PAK, Cla4. *J. Cell Biol.* **164**, 701–715.
20. Kinoshita, M., Kumar, S., Mizoguchi, A., Ide, C., Kinoshita, A., Haraguchi, T., Hiraoka, Y., and Noda, M. (1997). Nedd5, a mammalian septin, is a novel cytoskeletal component interacting with actin-based structures. *Genes Dev.* **11**, 1535–1547.
21. Takizawa, P.A., DeRisi, J.L., Wilhelm, J.E., and Vale, R.D. (2000). Plasma membrane compartmentalization in yeast by messenger RNA transport and a septin diffusion barrier. *Science* **290**, 341–344.